

Quantifying Jump Height Using Markerless Motion Capture with a Single Smartphone

Timilehin B. Aderinola*, Hananeh Younesian, Darragh Whelan,
Brian Caulfield, Georgiana Ifrim

Abstract—Goal: The countermovement jump (CMJ) is commonly used to measure the explosive power of the lower body. This study evaluates how accurately markerless motion capture (MMC) with a single smartphone can measure bilateral and unilateral CMJ jump height. **Methods:** First, three repetitions each of bilateral and unilateral CMJ were performed by sixteen healthy adults (mean age: 30.87 ± 7.24 years; mean BMI: $23.14 \pm 2.55 \text{ kg/m}^2$) on force plates and simultaneously captured using optical motion capture (OMC) and one smartphone camera. Next, MMC was performed on the smartphone videos using OpenPose. Then, we evaluated MMC in quantifying jump height using the force plate and OMC as ground truths. **Results:** MMC quantifies jump heights with MAE between 1.47 and 2.82 cm, and ICC between 0.84 and 0.99 without manual segmentation and camera calibration. **Conclusions:** Our results suggest that using a single smartphone for markerless motion capture is feasible.

Index Terms—Countermovement jump, Markerless motion capture, Optical motion capture, Jump height.

Impact Statement—Countermovement jump height can be accurately quantified using markerless motion capture with a single smartphone, with a simple setup that requires neither camera calibration nor manual segmentation.

I. INTRODUCTION

The countermovement jump (CMJ) is commonly used to measure lower-body explosive power and is characterized by an initial downward movement

of the center of mass (COM), known as *counter-movement*, before toe-off [1]. Performance assessment with CMJ often involves motion capture and measurement of metrics such as peak velocity and vertical jump height. Traditionally, motion capture is performed using wearable sensors, expensive optical motion capture (OMC) equipment and force plates. Although force plates and OMC are highly accurate, they are expensive, not readily portable, and their operation requires specialized knowledge. In addition, OMC requires physical body markers, which can be affected by skin and clothing artifacts. Moreover, wearable sensors, physical markers, and the awareness of being under observation may alter the real performance of subjects [2, 3].

Recent advances in computer vision research have enabled *markerless motion capture* (MMC) from videos. MMC often relies on human pose estimation (HPE) algorithms such as AlphaPose [4], OpenPose [5], and DeepLabCut [6]. These MMC techniques have shown potential to replace OMC, especially since smartphones are ubiquitous. However, there is still a lot to be done in evaluating the accuracy and usability of MMC.

Existing MMC approaches can be categorized based on *capture plane* (2D or 3D) and *number of cameras* (multi- or single-camera). 2D monocular (single-camera) techniques have been used for quantifying limb kinematics during underwater running [7] and sagittal plane kinematics during vertical jumps [8]. However, these works rely on deep learning approaches, where the generalization ability depends on the size and diversity of the data and the model architecture. For example, trained athletes, casual trainers, and rehabilitation patients will exhibit different performance ranges. Since collecting large quantities of representative data is difficult,

This work was funded by Enterprise Ireland under grant number IP20210963E and Science Foundation Ireland through the Insight Centre for Data Analytics (12/RC/2289_P2).

T.B. Aderinola, H. Younesian, B. Caulfield, and G. Ifrim are with the Insight SFI Centre for Data Analytics, University College Dublin, Ireland. D. Whelan is with Output Sports, NovaUCD, University College Dublin, Ireland. *Corresponding author. Email: timi.aderinola@insight-centre.org.

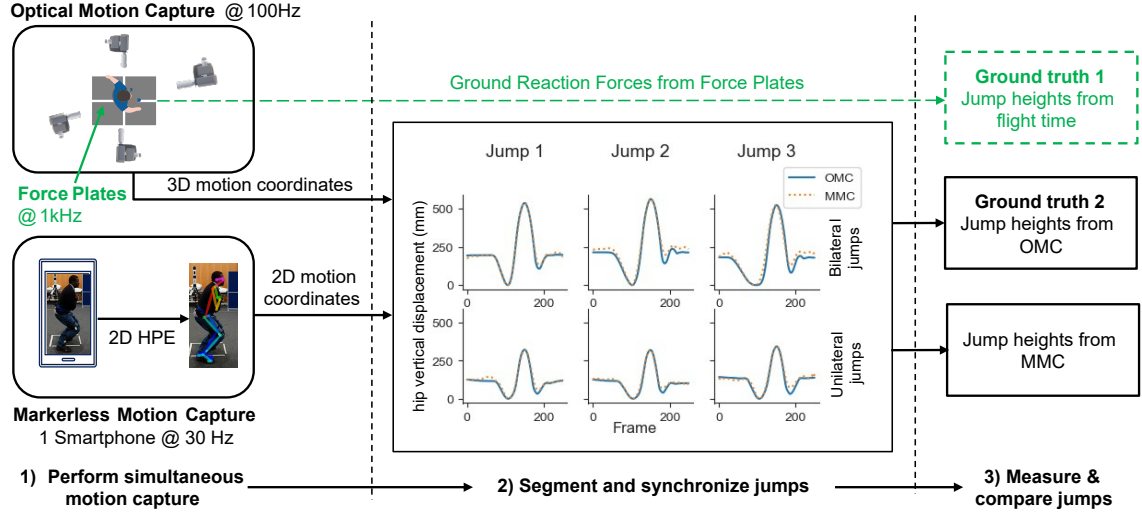


Fig. 1. Experiment setup showing simultaneous motion capture, preprocessing, and comparison with ground truths.

we take an alternative approach here, a quantitative approach, and we focus on the ease of deployment in practice and ease of use. The *My Jump2* app has been deployed for measuring jump height using a single smartphone. However, it requires manual selection of jump start and end frames [9]. Some other studies perform 3D MMC using multiple cameras [10, 11]. However, the 3D multi-camera approach requires careful calibration and reconstruction of 3D poses from multiple 2D camera angles, which is not feasible for wide deployment in practice.

Therefore, this study evaluates how accurately a single-smartphone-based MMC can measure bilateral and unilateral countermovement jump height. **Our main contributions are:**

- 1) We use a simple setup with a single smartphone, with no strict requirements on view perpendicularity and subject's distance from the camera. This is a more realistic application setting where MMC is used outside the lab, without specialized equipment.
- 2) We show how to exploit gravity as reference for pixel-to-metric conversion as proposed in [12], removing the need for reference objects or manual calibration.
- 3) We analyze how accurately MMC measures jump heights compared with OMC and force

plates.

- 4) We propose use cases of MMC depending on domain-specific accuracy requirements.

II. MATERIALS AND METHODS

A. Participants

Sixteen healthy adults (mean age: 30.87 ± 7.24 years; mean BMI: $23.14 \pm 2.55 \text{ kg/m}^2$) volunteered to participate in this study. The dominant foot of each participant was determined based on the foot with which they kick a ball [13]. Each participant signed the informed consent form approved by the Human Research Ethics Committee of University College Dublin with Research Ethics Reference Number LS-C-22-117-Younesian-Caulfield.

B. Tasks

After a five-minute warm-up, each participant performed three repetitions each of CMJ bilateral (BL) and unilateral (UL) while simultaneous motion capture was performed using force plates, OMC, and MMC (Fig. 1).

C. Apparatus

1) *Force Plate*: Force plates sampling at 1000 Hz are used as the first ground truth. To obtain the

flight time T_f for each jump, we first selected the flight phases using a threshold of $<5\%$ of the resting force. We then obtained T_f by differentiating the flight phases with respect to time. We obtain the jump height in centimeters as

$$h = 100gT_f^2/8 \quad (1)$$

where g is the acceleration due to gravity [14].

2) *Optical Motion Capture*: Optical motion capture was performed using four synchronized CODA¹ 3D cameras sampling at 100 Hz. Four clusters, each consisting of four light-emitting diode (LED) markers, were placed on the left and right lateral sides of the thigh and shank (Fig. 2). Moreover, six LED markers were placed on the anterior superior iliac crest (anterior and posterior), and greater trochanter (left and right). Three LED markers were attached to the lateral side of the calcaneus and on the first and fifth metatarsals of the dominant foot.

For a motor task with duration T seconds and K tracked joints, CODA outputs a sequence of 3D coordinates $\{(x_i^t, y_i^t, z_i^t) | i = 1, \dots, K; t = 1, \dots, 100T\}$ in *millimeters*; where z is the vertical axis, and 100 is the sampling rate.

3) *Markerless Motion Capture*: Markerless motion capture was performed in the side view using one Motorola G4 smartphone camera with a resolution of 720p and a frame rate of 30 frames per second (fps). The smartphone was placed on a tripod perpendicular to the dominant foot of the participant. We placed no strict requirements on camera view perpendicularity and distance to the participant. However, we ensured that the camera remained stationary and participants remained fully visible in the camera view.

To obtain motion data from the recorded videos, we performed 2D HPE using OpenPose [5]. The HPE algorithm outputs a sequence $\{(x_i^t, y_i^t, c_i^t) | i = 1, \dots, K; t = 1, \dots, 30T\}$, where 30 is the frame rate, (x_i^t, y_i^t) are the 2D coordinates in *pixels*, and $c_i^t \in [0, 1]$ is the probability for joint i in frame t .

D. Data Preprocessing

During preprocessing, we performed denoising, segmentation, resampling, and rescaling.

¹Charnwood Dynamics, UK (<https://codamotion.com>)

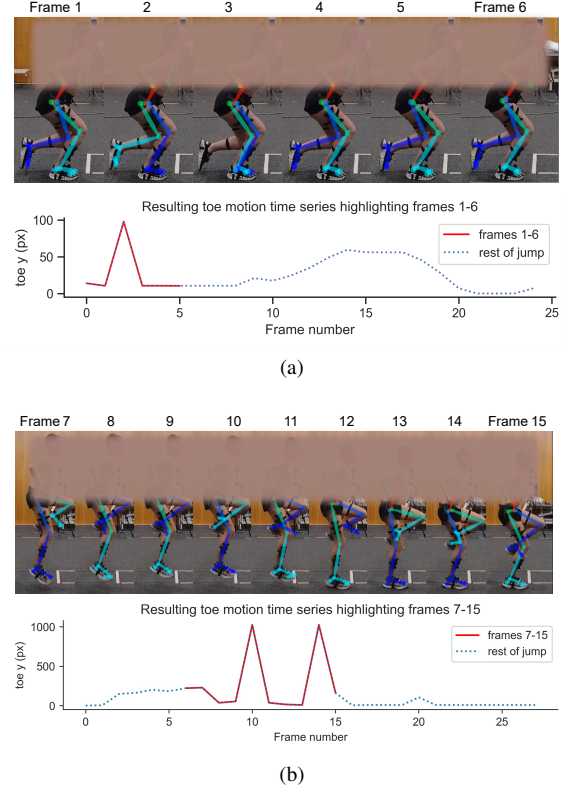


Fig. 2. Examples of noise in unilateral jumps during pose estimation as seen by observing the limb heatmap colors. (a) In frame 2, the left and right limbs are swapped. In frame 3, the right limb is wrongly detected as two limbs. (b) A failure case showing movements that are not characteristic of countermovement jumps.

1) *Denoising*: As shown in Fig. 2(a), occasional false detections in pose estimation appear as spikes on the motion time series. In most cases, these spikes could be removed by smoothing. However, 19 unilateral jumps such as Fig. 2(b) showed uncharacteristic movements and were removed as failure cases. To avoid filtering out important motion data, we performed smoothing of the OMC and MMC time series using z-score smoothing [15], proposed specifically for spike removal in motion sequences, and a second-order Savitzky-Golay [16] (Savgol) filter. The Savgol filter is known to smooth data with little distortion [17], and we chose a window size of 21 to preserve the main maxima and minima of the time series for accurate segmentation.

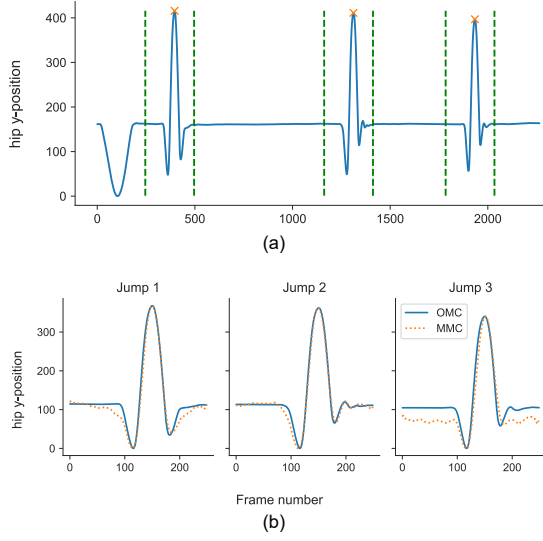


Fig. 3. Segmentation of jumps repetitions. (a) Raw hip vertical motion signal with peaks and selected jump windows. (b) Segmented and synchronized jumps based on selected windows.

2) *Segmentation and Resampling*: Each jump repetition is characterized by a dominant peak corresponding to the maximum vertical height attained by the hip (Fig. 3). Using these peaks as reference, we segmented each jump with a window t secs to either side of each peak, where t is based on exercise duration and capture frequency. This enabled synchronization of OMC and MMC based on start and stop times for each task. After segmentation, we upsample the MMC time series to match the length of the OMC time series using Fast Fourier Transform (FFT) resampling [18], which minimized distortion.

3) *Rescaling*: Two approaches were taken to rescale MMC from pixels (px) to a metric scale, namely *reverse minmax* (RMM) and *pixel-to-metric* (PTM).

Reverse MinMax (RMM) involved using OMC as reference to rescale MMC into metric mm . This was done by applying MinMax on both OMC and MMC, and then rescaling MMC into mm using the scaling factor obtained from OMC. Let vectors \mathbf{p}_{mm} and \mathbf{q}_{px} represent the OMC (in mm) and MMC (in px) time series respectively. We obtained $\mathbf{q}^* =$

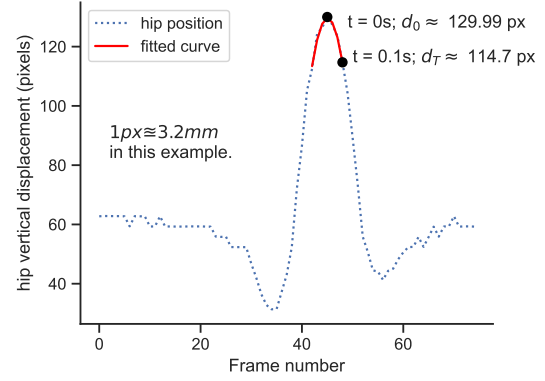


Fig. 4. Converting *pixel* to *millimetre* metric scale using gravity as reference.

$\text{MINMAX}(\mathbf{q})$, where $\mathbf{q}_i^* \in [0, 1]$, as

$$\mathbf{q}^* = \left\{ \frac{\mathbf{q}_{px_i} - \text{MIN}(\mathbf{q}_{px})}{\text{MAX}(\mathbf{q}_{px}) - \text{MIN}(\mathbf{q}_{px})} \right\} \quad (2)$$

where $i = 1, \dots, N$, and N is the length of \mathbf{q} . We then obtained \mathbf{q}_{px} in mm scale as

$$\mathbf{q}_{mm} = \{ \mathbf{q}_i^* [\text{MAX}(\mathbf{p}_{mm}) - \text{MIN}(\mathbf{p}_{mm})] + \text{MIN}(\mathbf{p}_{mm}) | i = 1, \dots, N \} \quad (3)$$

Since RMM requires OMC as reference, it can be used for evaluation purposes only.

Pixel-to-Metric (PTM) Conversion was performed based on the ‘free-fall’ of the centre of mass during a vertical jump. PTM uses g , the universal acceleration due to gravity as reference as proposed in [12]. From Newton’s law of motion, the motion of a rigid body² in free fall is described by

$$d(t) = d_0 + v_0 t + \frac{1}{2} g t^2 \quad (4)$$

where d_0 is the initial position in *metres* (m), v_0 is the velocity in m/s , and t is the elapsed time in *seconds* ($secs$). We set the free-fall duration, T , to depend on total hip vertical displacement, such that the hip’s non-free-fall motion is not captured.. At the peak, $v_0 = d_0 = 0$ (Fig. 4). After T secs free fall, $d_T = (500T^2g)mm$, such that

$$(500T^2g)mm = |d_0 - d_T|px \quad (5)$$

²Although the human body is not perfectly rigid, the deformations around the centre of mass are negligible in this instance.

Hence, 1 pixel $\equiv \mathcal{R}$ mm, where:

$$\mathcal{R} = \frac{500T^2g}{|d_0 - d_T|} \quad (6)$$

From this, we obtained \mathbf{q}_{mm} in mm scale as

$$\mathbf{q}_{mm} = \{\mathcal{R}(\mathbf{q}_{px_i}) | i = 1, \dots, N\} \quad (7)$$

E. Quantifying Jump Height

We measure jump heights directly from the OMC and the rescaled MMC time series as the maximum vertical displacement of the fifth metatarsal (toe_{vd}). We believe this approach is more straightforward than basing measurements on the flight time of the centre of mass (COM_{ft}), and we show in Section III-A that COM_{ft} overestimates jump heights by taking into account the motion of the hip before toe-off.

III. RESULTS

The jump height reported for each participant is the mean of all three repetitions performed for each task (Table I). Each MMC measurement was obtained using the reverse-minmax (RMM) and pixel-to-metric (PTM) approaches as described in Section II-D3. The mean \mathcal{R} across all the participants was 3.43mm/px. In cases of errors like the one shown in Fig. 2, the mean value of $\mathcal{R} = 3.43$ was used.

Section III-A compares jump heights obtained based on the flight time of the COM with jump heights obtained from the vertical displacement of the toe. Section III-B presents an evaluation of MMC accuracy using OMC and Force Plate as ground truths.

A. Measuring Jump Height: COM vs Toe

The flight time of the COM (COM_{ft}) is commonly used in estimating vertical jump height. In this section, we compare the differences in jump heights obtained by using COM_{ft} , and those obtained directly from the toe vertical displacement (toe_{vd}), both measured from OMC. Table II shows that, compared to toe_{vd} , COM_{ft} overestimates jump heights with absolute errors six times greater for bilateral jumps, and four times greater for unilateral jumps.

B. Comparative Analysis

We consider all jump repetitions from all participants as individual measurements, thereby recording 6 jumps per participant and 96 jumps in total, of which 77 (48 bilateral and 29 unilateral) were valid and used for analysis. Fig. 5 shows qualitatively how much MMC agrees with the Force Plate and OMC.

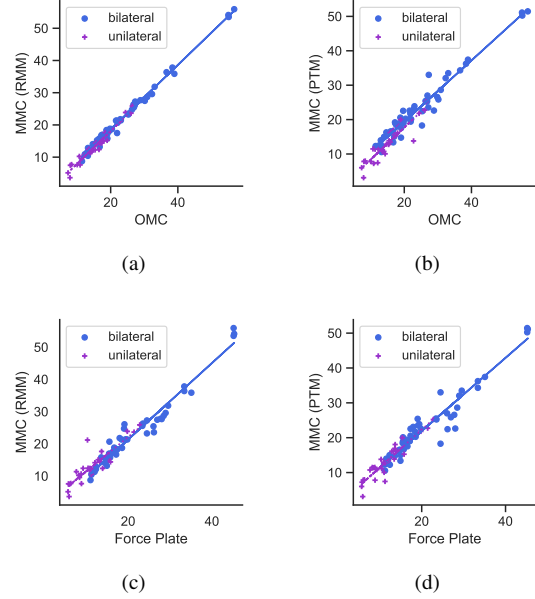


Fig. 5. Correlation between (a) OMC and MMC (RMM); (b) OMC and MMC (PTM); (c) Force Plate and MMC (RMM); and (d) Force Plate and MMC (PTM) for jump height measurement. Best viewed in color. Each datapoint in each scatterplot represents a single jump repetition.

For quantitative comparison (Table III), we use the Mean Absolute Error (MAE), intraclass correlation coefficient [20] (ICC), and Bland-Altman analysis [21] (BA). ICC and BA are often used for comparing new methods of measurements with a gold standard [9, 19]. The ICC has also been used to check for consistency and agreement across different methods of measuring jump height [22]. We take the simultaneous capture of each jump by FP, OMC, PTM and RMM each as a “trial”. We then compute ICC for four pairs of ‘trials’: OMC vs RMM, OMC vs PTM, FP vs RMM, and FP vs PTM, where FP and OMC are taken as ground truths. The $ICC \in [0, 1]$ gives the consistency of PTM and RMM with the ground truths, where a value closer to 1

TABLE I
JUMP HEIGHTS FROM FORCE PLATE, OMC, AND MMC

ID	Mean bilateral jumps (cm)				Mean unilateral jumps (cm)			
	FP	OMC	RMM	PTM	FP	OMC	RMM	PTM
P01	23.81	26.95	26.37	27.91	14.32	17.93	15.06	18.09
P02	11.81	12.58	10.96	12.43	8.64	10.68	8.60	9.60
P03	16.46	18.49	17.51	18.86	11.06	13.70	11.51	10.12
P04	18.19	21.54	20.52	21.54	E	E	E	F
P05	15.79	16.15	15.48	17.37	10.01	16.57	15.33	11.94
P06	15.88	17.64	16.76	19.35	8.22	10.68	10.24	11.48
P07	11.73	13.10	11.50	13.79	7.56	10.28	9.19	9.72
P08	13.70	15.63	12.80	12.99	5.88	7.73	5.41	5.65
P09	18.71	25.45	24.19	24.01	E	E	E	F
P10	18.50	20.24	19.49	20.62	12.10	16.39	13.81	14.10
P11	28.99	32.09	30.03	31.39	E	E	E	F
P12	15.15	20.99	17.98	18.10	6.72	12.42	9.47	8.99
P13	26.93	28.96	26.90	26.47	15.80	17.37	14.38	15.26
P14	33.96	37.99	36.68	35.99	13.43	16.01	14.35	15.67
P15	45.22	55.65	54.51	50.94	21.33	25.64	24.45	23.25
P16	26.22	26.50	24.82	21.12	E	E	E	F
Mean	21.32±8.80	24.37±10.56	22.91±10.64	23.31±9.52	11.54±4.19	14.58±4.61	12.62±4.66	12.82±4.55

F: Failure cases (Fig. 2). E: The corresponding FP, OMC, and RMM unilateral jumps are excluded from analysis.

TABLE II
JUMP HEIGHTS FROM COM VS. JUMP HEIGHTS FROM TOE USING OPTICAL MOTION CAPTURE

ID	Mean bilateral jumps (cm)			Errors (cm)		Mean unilateral jumps (cm)			Errors (cm)	
	FP	COM_{ft}	toe_{vd}	COM_{ft}	toe_{vd}	FP	COM_{ft}	toe_{vd}	COM_{ft}	toe_{vd}
P01	23.81	40.94	26.95	17.13	3.14	14.32	32.3	17.93	17.98	3.61
P02	11.81	40.17	12.58	28.36	0.77	8.64	25.41	10.68	16.77	2.04
P03	16.46	29.01	18.49	12.55	2.03	11.06	27.84	13.7	16.78	2.64
P04	18.19	31.28	21.54	13.09	3.35	6.93	18.95	9.35	12.02	2.42
P05	15.79	35.14	16.15	19.35	0.36	10.01	28.37	16.57	18.36	6.56
P06	15.88	31.71	17.64	15.83	1.76	8.22	22.61	10.68	14.39	2.46
P07	11.73	30.68	13.1	18.95	1.37	7.56	20.91	10.28	13.35	2.72
P08	13.7	30.6	15.63	16.9	1.93	5.88	17.25	7.73	11.37	1.85
P09	18.71	38.74	25.45	20.03	6.74	7.24	23.46	14.57	16.22	7.33
P10	18.5	32.4	20.24	13.9	1.74	12.1	27.54	16.39	15.44	4.29
P11	28.99	73.26	32.09	44.27	3.1	13.87	41.31	17.38	27.44	3.51
P12	15.15	27.42	20.99	12.27	5.84	6.72	16.63	12.42	9.91	5.7
P13	26.93	57.23	28.96	30.3	2.03	15.8	42.52	17.37	26.72	1.57
P14	33.96	78.12	37.99	44.16	4.03	13.43	36.72	16.01	23.29	2.58
P15	45.22	87.45	55.65	42.23	10.43	21.33	41.53	25.64	20.2	4.31
P16	26.22	51.59	26.5	25.37	0.28	9.51	33.32	11.07	23.81	1.56
Mean	21.32	44.73	24.37	23.42	3.06	10.79	28.54	14.24	17.75	3.45
	±8.80	±18.65	±10.56	±10.96	±2.58	±4.02	±8.38	±4.31	±5.14	±1.71

means higher consistency. While a high ICC does not necessarily mean close agreement, it shows the level of consistency of deviations from the ground truth. We obtain the ICC using the Pingouin [23] *intraclass_corr* module.

The Bland-Altman analysis is often used in clinical settings to visualize the agreement between two different methods of quantifying measurements based on bias and limits of agreement (LOA) [24]. The bias b for each MMC measurement technique

compared to ground truth is given by the mean of the differences between individual measurements. The LOA is obtained from the confidence interval, defined as $c_0 = b - 1.96SD$ and $c_1 = b + 1.96SD$, where SD is the standard deviation of the differences between the two measurements. At least 95% of joint positions measured with MMC will deviate from OMC by a value within the range $[c_0, c_1]$. We define $LOA = (c_1 - c_0)/2$, where a smaller LOA means better agreement with ground truth.

TABLE III
COMPARATIVE ANALYSIS AND BENCHMARK

	Method	Ground Truth	Segmentation	Calibrate?	MAE (cm)	ICC	bias (cm)	LOA (cm)
SoTA ¹ (Bilateral)	MMC [19]	OMC	Auto	Yes	-	0.68	0.15	2.75
	MyJump2 [9]	Force Plate	Manual	Yes	-	0.96	-0.48	2.13
Ours (Unilateral)	MMC _{RMM}	OMC	Auto	No	1.99	0.91	1.99	2.13
	MMC _{PTM}	OMC	Auto	No	2.13	0.86	1.96	4.05
	MMC _{RMM}	Force Plate	Auto	No	2.08	0.84	-1.54	4.7
	MMC _{PTM}	Force Plate	Auto	No	2.21	0.87	-1.57	3.8
Ours (Bilateral)	MMC _{RMM}	OMC	Auto	No	1.47	0.99	1.47	1.86
	MMC _{PTM}	OMC	Auto	No	2.02	0.97	1.07	4.80
	MMC _{RMM}	Force Plate	Auto	No	2.09	0.93	-1.59	5.40
	MMC _{PTM}	Force Plate	Auto	No	2.82	0.93	-1.99	5.45
Ours (BL and UL)	MMC _{RMM}	OMC	Auto	No	1.66	0.98	1.66	2.05
	MMC _{PTM}	OMC	Auto	No	2.07	0.96	-1.41	4.60
	MMC _{RMM}	Force Plate	Auto	No	2.09	0.95	-1.57	5.15
	MMC _{PTM}	Force Plate	Auto	No	2.59	0.95	-1.83	4.90

¹State of the art as reported in the respective works. MAE (Mean Absolute Errors) are not reported in these works.

BL: bilateral; UL: unilateral; RMM: reverse minmax; PTM: pixel-to-metric. Best value for each metric is shown in **bold** font face.

We perform Bland-Altman analysis using statsmodels [25]. Based on ICC, bias, and LOA, and simplicity of setup, we put this work in context with similar approaches (Table III).

1) *MMC vs OMC*: First, the accuracy of MMC in quantifying jump height is evaluated with OMC as ground truth. Unlike in Section III-A, both MMC and OMC are measured using the vertical displacement of the toe in this instance. As shown in Table III, both MMC_{RMM} and MMC_{PTM} achieve results comparable with the work of [19], which was also evaluated using OMC equipment. It is worth noting that our PTM approach assumes a simpler setup without manual calibration.

2) *MMC vs Force Plate*: The jump height measured from the force plates is taken as the main ground truth in this section. As shown in Table III, MMC_{RMM} and MMC_{PTM} fall short of the results achieved with MyJump2 [9], especially during unilateral jumps. This is because the MyJump2 app involves manual selection of start and end frames of jumps, and also requires subjects to be 1m away from the camera. In addition, effective usage of MyJump2 may also require a second party holding the camera. On the other hand, our methods are simpler and more convenient, requiring only a tripod stand and one calibrating jump.

IV. DISCUSSION

In this study, we have evaluated the accuracy of 2D markerless motion capture with a single smartphone in quantifying vertical jump height during

countermovement jumps. Optical motion capture (OMC) was performed using CODA, and markerless motion capture (MMC) was performed using OpenPose with a single smartphone camera. Jump heights obtained from force plate flight times were used as the first ground truth for evaluating jump height, while OMC was used as the second ground truth. We found that MMC can quantify jump heights with MAE between 1.47 and 2.82 cm without manual segmentation and camera calibration. We also obtained ICC between 0.84 and 0.99. The greatest agreement is found between OMC and MMC_{RMM} (LOA between 1.86 cm and 5.40 cm) because Reverse MinMax is performed based on OMC. On the other hand, MMC_{PTM} is more prone to errors (LOA between 3.8 cm and 5.45 cm) since noise in the jump time series is further amplified by the pixel-to-metric conversion factor, \mathcal{R} .

Although our proposed methods achieve comparable results, the acceptability of LOA will depend on measures similar to the *minimally important difference* [26] (MID) in each application context. In order to be acceptable, the LOA should be smaller than the MID. For example, the MID in an elite sports context would be considerably smaller than the MID in recreational athletes.

There are some limitations to this approach. For example, the pixel-to-metric conversion requires a calibrating jump, and movements towards or away from the camera during each task change the pixel-to-metric scale. In general, the main sources of error we identify in MMC are:

- 1) Video quality. The quality of the video and the amount of clutter in the background affect the confidence of detected keypoints during pose estimation.
- 2) Video viewpoint. Accurate detection of body parts is affected by video viewpoint. For example, pose estimation sometimes fails when used for unilateral CMJ in the side view (Fig. 2). Future studies will explore other views for the unilateral CMJ.
- 3) Noise in HPE output. The noise level could be influenced by HPE model accuracy, background clutter, and lighting conditions.
- 4) Approximations. Preprocessing steps such as smoothing, segmentation, MMC scaling and pixel-to-metric conversion involve approximations, introducing errors.

The Force Plate and OMC are also prone to errors due to human factors. For example, OMC coordinates drop to zero when participants' hands or clothes occlude markers. Force values are also affected if participants step outside the force plates momentarily.

V. CONCLUSION

The results of the analyses in this study suggest that markerless motion capture with a single smartphone is feasible. However, its use case will depend on the domain-specific minimally important differences (MID). For example, for applications with very small MID, monocular MMC could provide enhanced feedback and/or augmentation for body-worn sensors and markers. On the other hand, for applications such as measuring countermovement jump height, MMC frame-by-frame tracking accuracy is not critical. Hence, as shown in this study, 2D monocular MMC could potentially replace sensors and physical markers for such applications.

This study focuses on two variants of one motor task with sixteen participants. Future studies will focus on improving and generalizing the techniques used to cover a comprehensive range of motor tasks. In addition, the videos used in this study were captured in the side view. Future studies will consider other views and their effects on capture techniques.

REFERENCES

- [1] L. Petrigna, B. Karsten, G. Marcolin, A. Paoli, G. D'Antona, A. Palma, and A. Bianco, "A review of countermovement and squat jump testing methods in the context of public health examination in adolescence: Reliability and feasibility of current testing procedures," *Frontiers in Physiology*, vol. 10, Nov 2019.
- [2] L. Wade, L. Needham, P. McGuigan, and J. Bilzon, "Applications and limitations of current markerless motion capture methods for clinical gait biomechanics," *PeerJ*, vol. 10, p. e12995, 2022.
- [3] C. L. Geh, M. R. Beauchamp, P. R. Crocker, and M. G. Carpenter, "Assessed and distressed: White-coat effects on clinical balance performance," *Journal of Psychosomatic Research*, vol. 70, no. 1, p. 45–51, Jan 2011.
- [4] H.-S. Fang, S. Xie, Y.-W. Tai, and C. Lu, "RMPE: Regional multi-person pose estimation," in *ICCV*, 2017.
- [5] Z. Cao, G. Hidalgo Martinez, T. Simon, S. Wei, and Y. A. Sheikh, "Openpose: Realtime multi-person 2d pose estimation using part affinity fields," *IEEE Transactions on Pattern Analysis and Machine Intelligence*, 2019.
- [6] A. Mathis, P. Mamidanna, K. M. Cury, T. Abe, V. N. Murthy, M. W. Mathis, and M. Bethge, "Deeplabcut: markerless pose estimation of user-defined body parts with deep learning," *Nature neuroscience*, vol. 21, no. 9, pp. 1281–1289, 2018.
- [7] N. J. Cronin, T. Rantalainen, J. P. Ahtiainen, E. Hynynen, and B. Waller, "Markerless 2d kinematic analysis of underwater running: A deep learning approach," *Journal of Biomechanics*, vol. 87, p. 75–82, 2019.
- [8] J. F. Drazen, W. T. Phillips, N. Seethapathi, T. J. Hullfish, and J. R. Baxter, "Moving outside the lab: markerless motion capture accurately quantifies sagittal plane kinematics during the vertical jump," *Journal of Biomechanics*, p. 110547, 2021.
- [9] Š. Bogataj, M. Pajek, V. Hadžić, S. Andrašić, J. Padulo, and N. Trajković, "Validity, reliability, and usefulness of my jump 2 app for measuring vertical jump in primary school chil-

- dren,” *International Journal of Environmental Research and Public Health*, vol. 17, no. 10, p. 3708, May 2020.
- [10] N. Nakano, T. Sakura, K. Ueda, L. Omura, A. Kimura, Y. Iino, S. Fukashiro, and S. Yoshioka, “Evaluation of 3d markerless motion capture accuracy using openpose with multiple video cameras,” *Frontiers in sports and active living*, vol. 2, p. 50, 2020.
- [11] S. Corazza, L. Mündermann, A. M. Chaudhari, T. Demattio, C. Cobelli, and T. P. Andriacchi, “A markerless motion capture system to study musculoskeletal biomechanics: Visual hull and simulated annealing approach,” *Annals of Biomedical Engineering*, vol. 34, no. 6, p. 1019–1029, 2006.
- [12] D. Bieler, S. Gunel, P. Fua, and H. Rhodin, “Gravity as a reference for estimating a person’s height from video,” in *Proceedings of the IEEE/CVF International Conference on Computer Vision (ICCV)*, October 2019.
- [13] N. van Melick, B. M. Meddeler, T. J. Hoogboom, M. W. G. Nijhuis-van der Sanden, and R. E. H. van Cingel, “How to determine leg dominance: The agreement between self-reported and observed performance in healthy adults,” *PLOS ONE*, vol. 12, no. 12, p. e0189876, Dec 2017.
- [14] G. L. Moir, “Three different methods of calculating vertical jump height from force platform data in men and women,” *Measurement in Physical Education and Exercise Science*, vol. 12, no. 4, pp. 207–218, 2008.
- [15] T. B. Aderinola, T. Connie, T. S. Ong, A. Beng, and K. O. M. Goh, “Gait-based age group classification with adaptive graph neural network,” *arXiv.org*, 2022. [Online]. Available: <https://arxiv.org/abs/2210.00294>
- [16] A. Savitzky and M. J. Golay, “Smoothing and differentiation of data by simplified least squares procedures,” *Analytical chemistry*, vol. 36, no. 8, pp. 1627–1639, 1964.
- [17] J. L. Guinón, E. M. Ortega, J. García-Antón, and V. Pérez-Herranz, “Moving average and savitzki-golay smoothing filters using mathcad,” 2007.
- [18] W. Hawkins, “Fourier transform resampling: theory and application [medical imaging],” in *1996 IEEE Nuclear Science Symposium. Conference Record*, vol. 3, 1996, pp. 1491–1495 vol.3.
- [19] F. Webering, H. Blume, and I. Allaham, “Markerless camera-based vertical jump height measurement using openpose,” in *Proceedings of the IEEE/CVF Conference on Computer Vision and Pattern Recognition (CVPR) Workshops*, June 2021, pp. 3868–3874.
- [20] S. P. JL, “Intraclass correlations: uses in assessing rater reliability,” *Psychological bulletin*, vol. 86, no. 2, 2021.
- [21] J. M. Bland and D. Altman, “Statistical methods for assessing agreement between two methods of clinical measurement,” *The lancet*, vol. 327, no. 8476, pp. 307–310, 1986.
- [22] G. L. Moir, “Three different methods of calculating vertical jump height from force platform data in men and women,” *Measurement in Physical Education and Exercise Science*, vol. 12, no. 4, pp. 207–218, 2008.
- [23] R. Vallat, “Pingouin: statistics in python,” *Journal of Open Source Software*, vol. 3, no. 31, p. 1026, Nov 2018.
- [24] D. Giavarina, “Understanding bland altman analysis,” *Biochemia Medica*, vol. 25, no. 2, p. 141–151, 2015.
- [25] S. Seabold and J. Perktold, “statsmodels: Econometric and statistical modeling with python,” in *9th Python in Science Conference*, 2010.
- [26] P. Carton and D. Filan, “Defining the minimal clinically important difference in athletes undergoing arthroscopic correction of sports-related femoroacetabular impingement: The percentage of possible improvement,” *Orthopaedic Journal of Sports Medicine*, vol. 8, no. 1, p. 232596711989474, 2020.